Fabrication of nitrogen-doped ultrananocrystalline diamond nanowire arrays with enhanced field emission and plasma illumination performance

Ting-Hsun Chang*
Department of Materials Science and Engineering
National Tsing-Hua University
Hsin-Chu 30013, Taiwan, China
s9831576@m98.nthu.edu.tw

Kamatchi Jothiramalingam Sankaran
Department of Materials Science and Engineering
National Tsing-Hua University
Hsin-Chu 30013, Taiwan, China
jothisankaran@gmail.com

Shiu-Cheng Lou
Department of Electro-Optical Engineering
Yuan-Tze University
Chung-Li 32003, Taiwan, China
cdsas6688@gmail.com

Chulung Chen
Department of Electro-Optical Engineering
Yuan-Tze University
Chung-Li 32003, Taiwan, China
chulung@saturn.yzu.edu.tw

Nyan-Hua Tai
Department of Materials Science and Engineering
National Tsing-Hua University
Hsin-Chu 30013, Taiwan, China
nhtai@mx.nthu.edu.tw

I-Nan Lin
Department of Physics
Tamkang University
New Taipei, 25137 Taiwan, China
inanlin@mail.tku.edu.tw

***Abstract*—Large-area silicon nanowire arrays (SiNAs) were fabricated via metal catalytic etching technique, in conjunction with the polystyrene spheres lithographic process. The nitrogen-doped ultrananocrystalline diamond (N_2-UNCD) films were coated on thus formed SiNA by using microwave plasma chemical vapor deposition (MPECVD) process. The N_2-UNCD/SiNWs films, which were grown in CH_4/N_2 plasma at 700°C, possess markedly better conductivity ($\sigma_{N2\text{-}UNCD}$=2-3(Ω cm)$^{-1}$) than the conventional c-UNCD/SiNWs films, which were grown in CH_4/Ar plasma at around 425°C (σ_{UNCD}=0.01(Ω cm)$^{-1}$). The EFE process of the former materials can be turned on at $(E_0)_{N2\text{-}UNCD}$=7.80 V/μm achieving larger EFE current density of $(J_e)_{N2\text{-}UNCD}$=0.67 mA/cm^2 at an applied field of 13.0 V/μm ,whereas that of the latter materials need $(E_0)_{=UNCD}$=18.25 V/μm to turn on, attaining only $(J_e)_{UNCD}$=0.024 mA/cm^2 at same applied field. While the plasma illumination process can be triggered at around 0.21 V/μm, regardless of the characteristics of the cathod materials, plasma illumination intensity/current density is larger when the materials with better EFE properties were used as cathodes for the plasma device. The plasma illumination current density is around $(J_{pi})_{N2\text{-}UNCD}$=5.0 mA/cm^2 (at an applied field of 0.35 V/μm) when N_2-UNCD/SiNWs film was used as cathode, whereas the $(J_{pi})_{UNCD}$=3.2 mA/cm^2 when the conventional UNCD/SiNWs film was used as cathode. In summary, it is observed that the plasma illumination charateristics of the CP-devices is closely correlated with the electron field emission behavior of the cathode materials, which, in turn, was enhanced due to the improvement in conductivity of the UNCD films.**

***Keywords*: silicon nanowire arrays (SiNAs), nitrogen-doped ultrananocrystalline diamond (UNCD)**

I. INTRODUCTION

Diamond films possess good electron field emission (EFE) properties, besides their marvelous physical and chemical properties, and can potentially be applied as material for fabricating electron field emitters [1-3]. There are substantial researches carried out on the growth, properties and applications of single crystalline and microcrystalline diamond (MCD) in the last few decades. Recently, main focus has been directed towards the synthesis and properties of ultra-nanocrystalline diamond (UNCD) films [4], as the UNCD films possess many excellent properties and several of them actually exceed those of diamond [5]. A very high electron field emission characteristic has been reported for UNCD films [6-8]. Among the potential application for the diamond electron field emitter, the electron source for the microcavity plasma devices looks more

promising. Microcavity plasma devices represent a new photonics technology at the interface of plasma science and optoelectronics in which a nonequilibrium plasma is spatially confined to cavities with cross-sectional dimensions as small as 10 μm [9-11]. These devices exhibit great potential for a broad spectrum of applications in materials synthesis, environmental sensing, and elemental analysis, as the microplasma devices are advantageous in (i) the power loading (of the order of kW cm^{-3}) and (ii) the ability to operate continuously at pressures up to and beyond 1 atm [12-16]. On the other hand, plasma display technology has advanced considerably in the past decade but faced the challenges of insufficient luminous efficiency of the plasma devices [17]. The development of a cathode material, which can efficiently emit the electrons for the purpose of improving the performance of a plasma illumination device, is thus called for.

In these studies, we utilized highly conducting UNCD films as coating materials to enhance the plasma illumination characteristics of the capacitive-type plasma devices (CP-devices) and observed marked enhancement in the plasma illumination characteristics of the CP-devices. The detail microstructure of these films was investigated using transmission electron microscopy (TEM) so as to elucidate the mechanism that improved the characteristics of the CP-devices.

II. Experimental

A nano-sphere based lithography technique was used to fabricate the Si-nanowire (SiNW) array templates. The (100) Si substrates were pre-cleaned by using a RCA process [18], which includes rinsing the Si wafer sequentially in water-diluted hydrogen peroxide/ammonium hydroxide and hydrogen peroxide/hydrochloric acid solution. The polystyrene spheres (PS) about 500 nm in diameter were firstly overlaid on the Si substrates by a drop-coating process (Fig. 1(a)). The closed packed PS layer was plasma etched (air, 50 watts) for a few minutes to shrink the size of PS sphere (Fig. 1(b)), followed by the deposition of a thin Ag film via sputter and the removable of PS sphere by ultrasonicating the Ag-coated substrate in deionized water to form a Ag mask with regularity arranged spherical pattern of exposed Si-surface (Fig. 1(c)). These Ag-patterned Si-substrates were then dip into an etching solution (HF (4.60 M)+H_2O_2 (0.44 M)) to etch away the Si underneath the Ag-coating will be etched away by a self-gavanic process

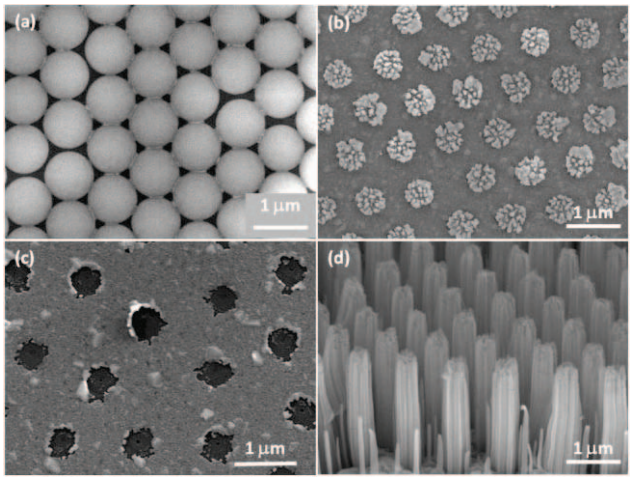

Fig. 1 The SEM micrographs showing the sequence of fabricating the SiNW templates: (a) PS coated, (b) Ar plasma etched, (c) Ag-coated and after PS removal and (d) SiNWs after etching in HF +H_2O_2 for 10 min.

[19], forming Si-NWs about 300 in diameter, which is the same size of the PS spheres. Thus formed SiNW arrays were thermal oxidized in air (1000°C, 10 min), followed by dipping in 10% HF solution for 1 min, to sharpen the SiNWs, resulting in a templates, which contain SiNWs about 300 nm in diameter, 2-3 μm in length (Fig. 1(d)). The UNCD films were then grown on these SiNW array templates. In the growth of highly conductive UNCD films, the plasma (CH_4/N_2=6/94) was excited by a microwave (2.45 GHz) of 1200 W in 50 torr total pressure. The substrates (SiNWs templates) were heated to 700°C by a resistance heater. The UNCD-coated SiNW nanostructures formed by such a MPECVD process for 10 min in designated as N_2-UNCD/SiNWs. To facilitate the comparison, conventional UNCD films were grown in CH_4/Ar=1/99 sccm plasma for 60 min by using a MPECVD process (2.45 GHz, 1200 W, 120 torr total pressure). The UNCD films were grown without external heater. Thus obtained samples were designated as c-UNCD/SiNWs.

The morphology of the as prepared and UNCD coated SiNW array templates was examined using field emission SEM (JEOL JSM-6500F). The bonding structure of the UNCD films coated on the SiNWs was investigated by a 632 nm Raman spectroscopy. The electron field emission (EFE) properties of the as-prepared and UNCD-coated SiNWs were measured using a parallel setup, in which the anode (W-rod, 1 mm in diameter) was separated from the cathode (UNCD-coated SiNW arrays) with the cathode-to-anode distance controlled by an adjustable micrometer attached to the anode. The current-to-votage characteristics of the UNCD-coated SiNW arrays

were acquired in a high vacuum environment (5×10^{-6} torr) by a Keitheley 237 and the current density vs applied field (J-E) curves were modeled by Fowler-Nordheim (F-N) model [20]. The turn-on field for inducing the EFE process was designated as the interception of the lines extrapolated from the low-field and high-field segments in F-N plots, which were in J/E^2 vs 1/E curves. The plasma illumination characteristics of a capacitive-type plasma device (CP-devices) were characterized by a parallel plate configuration, in which the Indium-Tin oxide (ITO) coated glass plates (the anode) was separated from the UNCD/SiNW arrays (the cathode) by a fixed spacer (teflon, 1.0 mm in thickness). The Ar plasma was excited in between the ITO and UNCD/SiNWs by applying a positive voltage pulsed (0~400 V) to the anode in a vacuum of ~100 torr. The current density vs. applied field of such a setup was acquired using a Keitheley 2410 current source electrometer.

III. Results and Discussion

The characteristics of the UNCD films grown on planar Si substrates were investigated first for the purpose of developing the most proper UNCD films for fabricating the UNCD/SiNW arrays. Figures 2(a) and 2(b) show the SEM morphology of the UNCD films grown in CH_4/N_2 and CH_4/Ar plasma, respectively, indicating that both UNCD films contain ultra-small grains with very smooth surface that is very promising for coating on the SiNW arrays conformally. The UNCD films grown in CH_4/N_2 plasma (N_2-UNCD) consist of acicular grains about 5 nm x 300 nm in size (Fig. 2(a)), whereas the films grown in CH_4/Ar plasma (c-UNCD) contain of equi-axed grains about 5 nm in size. Detail examinations using transmission electron microscopy (TEM) reveals a unique granular structure for the CH_4/N_2-plasma derived N_2-UNCD films, as compared with the conventional c-NCD films grown in CH_4/Ar plasma. Figure 3(a) and the corresponding inset show that the N_2-UNCD films consist of needle like diamond grains about 5 nm in diameter and a few hundreds of nanometer in length. In contrast, Fig. 3(b) and the inset show that the c-UNCD films contain spherical diamond grains about 5 nm in size. Moreover, structure image in TEM (not shown here) revels that each needle-like diamond grains were encased with a thin layer of graphitic phase. The significance of such a unique granular structure on the electron field emission and plasma illumination behavior of the materials will be discussed shortly.

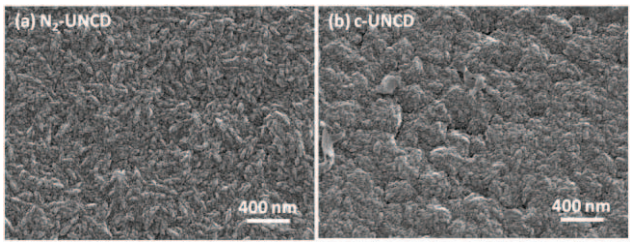

Fig. 2 The SEM micrographs of the UNCD films grown on planar Si-substrates: (a) N_2-UNCD films grown in CH_4/N_2 plasma at 700°C for 10 min and (b) conventional c-UNCD films grown in CH_4/Ar plasma at around 425°C for 60 min.

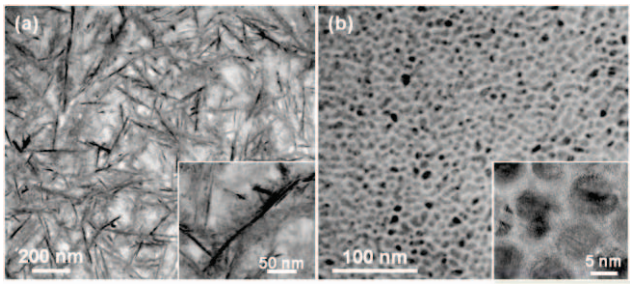

Fig. 3 The TEM micrographs of the UNCD films grown on planar Si-substrates: (a) N_2-UNCD films grown in CH_4/N_2 plasma at 700°C for 10 min and (b) conventional c-UNCD films grown in CH_4/Ar plasma at around 425°C for 60 min.

Raman spectroscopy shown in Fig. 4 shows that both N_2-UNCD/SiNWs and c-UNCD/SiNWs contain broaden Raman resonance peaks, which characterize UNCD films with ultrasmall grain size [4]. Both Raman spectra contain D*-band (1350 cm^{-1}) and G-band (1580 cm^{-1}) resonance peaks, which represent disordered carbon [21] and amorphous carbon (a-C) (or graphitic) phase [22], respectively. There also presents a small diffuse Raman resonance peaks near 1140 cm^{-1} and 1480 cm^{-1} which represent trans-polyacetylene along the grain boundaries [23,24]. Moreover, the N_2-UNCD/SiNWs films have G*-band appears at 1600 cm^{-1}, which imply that there exists nano-crystalline graphitic phase. Such an observation is in accord with the TEM microstructural investigation. Moreover, the c-UNCD/SiNWs films show slightly larger G-band/D-band ratio than the N_2-UNCD/SiNWs films, indicating that the CH_4/Ar plasma based MPECVD process results in larger proportion of a-C phase.

Four point measurements show that, when directly grown in planar Si substrates, the planar N_2-UNCD films possess a conductivity as good as $\sigma_{N2\text{-}UNCD}$=2-3 $(\Omega\ cm)^{-1}$, whereas the

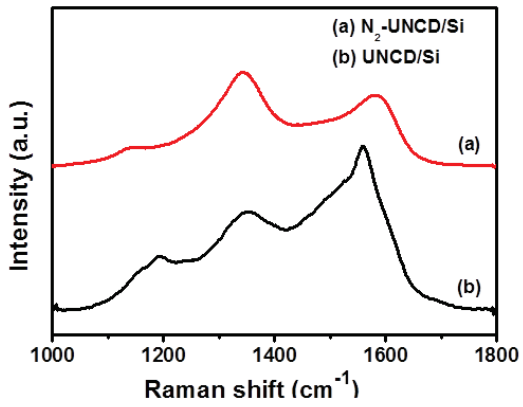

Fig. 4 The Raman spectrascopy of the UNCD films coated on the planar Si substrates: (a) N_2-UNCD films grown in CH_4/N_2 plasma at 700°C for 10 min and (b) conventional UNCD films grown in CH_4/Ar plasma at around 425°C for 60 min.

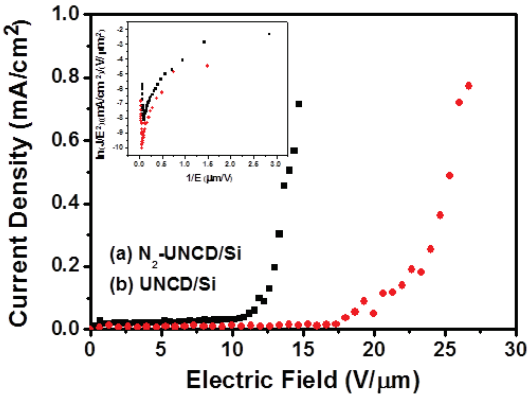

Fig. 5 The electron field emission properties of the UNCD films coated on the planar Si substrates: (a) N_2-UNCD films grown in CH_4/N_2 plasma at 700°C for 10 min and (b) conventional UNCD films grown in CH_4/Ar plasma at around 425°C for 60 min.

conductivity the conventional c-UNCD films is two order of magnitude smaller (i.e., $\sigma_{UNCD} \leq 0.01(\Omega\text{-cm})^{-1}$). Hall measurement using Van der Pauw configuration reveal that plasma N_2-UNCD films possess n-type conductivity, i.e., electron concentration of $n=2.0 \times 10^{22}$ cm^{-3} and the electrical conductivity of 186 $(\Omega\text{-cm})^{-1}$ (the Hall coefficient is not measurable for plasma UNCD films). Figure 5(a) shows the EFE properties of thus grown UNCD films, indicating that the N_2-UNCD films exhibit much better electron field emission (EFE) properties then the conventional c-UNCD films do. The EFE process for the N_2-UNCD films can be turned on at a field of $(E_0)_{N2\text{-}UNCD}$ =10.87 V/μm, attaining a EFE current density of $(J_e)_{N2\text{-}UNCD}$= 0.75 mA/cm^2 at an applied field of 14.7 V/μm (curve I, Fig. 5(a)). In contrast, curve II in Fig. 5(a) shows that the c-UNCD/SiNW films requires markedly larger field to turn on the EFE process ($(E_0)_{c\text{-}UNCD}$=17.5 V/μm) and the EFE current density can only attain $(J_e)_{c\text{-}UNCD}$=0.013 mA/cm^2 at the same applied field. It needs markedly larger applied field (E_a=27.0 V/μm) to attain the same lagre EFE current density (0.75 mA/cm^2). The superior EFE properties for the N_2-UNCD films, as compared with those for conventional c-UNCD films, are apparently resulted from the better conductivity for the former. The electronic properties of these planar UNCD films were summarized in Table I(a).

Both the N_2-UNCD and c-UNCD films were then used for coating the SiNW arrays to develop the cathode materials for inducing the plasma in the CP-devices. The morphology of the UNCD coated SiNWs was shown in Fig. 6, with the insets showing the enlarged micrographs of the UNCD-coated SiNWs.

TABLE I. The EFE properties for the UNCD films grown on the planar Si substrates and the Si-nanowire array templates (UNCD/SiNWs)

materials		conductivity $(\Omega\text{-cm})^{-1}$	Electron field emission		Plasma illumination	
			E_0 (V/μm)	J_e (μA/cm^2)	E_{th} (V/μm)	J_{pl} (μA/cm^2)
(a)	c-UNCD films	≤0.01	17.50	<12.7	-	-
	N_2-UNCD films	2-3	10.87	303.0	-	-
(b)	SiNWs	-	31.57	23.0	0.24	2.0
	c-UNCD/SiNWs	-	18.25	24.0	0.21	3.2
	N_2-UNCD/SiNWs	-	7.8	870.0	0.21	5.0

E_0: the turn-on field derived from Fowler-Nordheim plots, as the interceptions of straight lines extrapolated from the low-field and high-field segments of the F-N plots.
J_e: the electron field emission current density achieved at applied field of E_a=13.0 V/ m for planar UNCD films in (a) and is E_a=13.0 V/μm for UNCD/SiNWs in (b).
E_{th}: the threshold field for triggering the plasma in the CP-devices.
J_{pl}: the plasma current density achieved in the CP-devices at applied field of E_{pl}=0.36 V/μm.

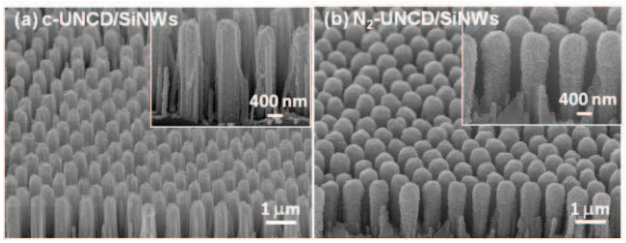

Fig. 6 The SEM micrographs of the diamond coated SiNW templates: (a) N_2-UNCD/SiNWs coated in CH_4/N_2 plasma at 700°C for 10 min and (b) conventional UNCD/SiNW coated in CH_4/Ar plasma at around 425°C for 60 min. The insets show the enlarged micrographs of the corresponding UNCD/SiNWs (the bars in the insets are 400 nm).

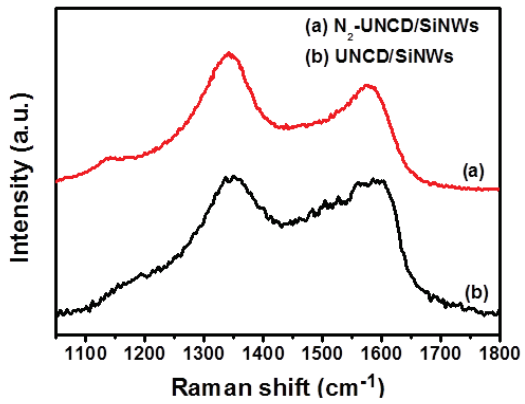

Fig. 7 The Raman spectrascopy of the UNCD films coated on the SiNW templates: (a) N_2-UNCD films grown in CH_4/N_2 plasma at 700°C for 10 min and (b) conventional UNCD films grown in CH_4/Ar plasma at around 425°C for 60 min.

These figures show that the UNCD films were conformally coated on SiNWs, regardless the constituent in the plasma. The growth of UNCD films in CH_4/N_2 plasma (at 700°C) is much faster such that N_2-UNCD films (300 nm in thickness) can completely cover the SiNWs by 10 min MPECVD process (Fig. 6(a)). In contrast, the growth of c-UNCD films is slower in CH_4/Ar plasma (without heating) such that it needs about 60 min MPECVD process to reach similar thickness (Fig. 6(b)). It is not clear whether it is the difference in plasma constituent or the substrate temperature that results in difference in growth rate for the UNCD films. But both films possess the same good crystallinity. Raman spectroscopy in Fig. 7 shows that both N_2-UNCD/SiNWs and c-UNCD/SiNW nanostructure materials possess broaden Raman resonance peaks, which are similar with the Raman spectroscopy of the planar UNCD films (cf. Fig. 4). Briefly, besides the disordered carbon (D*-band, 1350cm^{-1}) and the graphitic (G-band, 1580 cm^{-1}) resonance peaks with large intensity, they contain trans-polyacetylene phase, υ_1-band (1140 cm^{-1}) and υ_2-band (1480 cm^{-1}), with smaller intensity.

Figure 8 shows that the EFE properties of thus obtained UNCD/SiNWs, indicating that the N_2-UNCD/SiNW nanostructure materials exhibit much superior to those of the conventional c-UNCD/SiNW ones. The EFE process for the N_2-UNCD/SiNWs films can be turned on at a field of $(E_0)_{N2\text{-}UNCD}$ =7.80 V/μm, attaining a EFE current density of $(J_e)_{N2\text{-}UNCD}$= 0.87 mA/cm^2 at an applied field of 13.0 V/μm (Fig. 8(a)). In contrast, Fig. 8(b) shows that it requires markedly larger field to turn on the EFE process for c-UNCD/SiNW nanostructure materials ($(E_0)_{UNCD}$=18.25 V/μm) and the EFE current density can only attain $(J_e)_{UNCD}$=0.024 mA/cm^2 at an applied field of 13.0 V/μm. It needs markedly larger applied field (E_a=32.0 V/mm) to attain an EFE current density of 0.8 mA/cm^2. The superior EFE properties for the N_2-UNCD/SiNW nanostructure materials, as compared with those for conventional c-UNCD/SiNW ones, is, presumably, resulted from the better conductivity for the N_2-UNCD nanostructure materials. Nevertheless, both N_2-UNCD and c-UNCD coated SiNW arrays show EFE properties significantly superior to the uncoated SiNW arrays, which possess trun-on field and EFE capacity of E_0=31.57 V/μm and J_e=0.024 mA/cm^2 at 13.0 V/μm, respectively, and and it requires E_a=50.0 V/μm to attain the same large EFE current density (0.87 mA/cm^2).

Usually, the materials in the nanowire geometry shows markedly better electron field emission properties than their thin film counterpart due to the presence of large field concentration factor in nanowire form. However, the benefit of high field enhancement factor for growing the UNCD films on SiNW array templates is not observable here. The EFE properties of the UNCD/SiNW arrays are only moderately better than those for the N_2-UNCD (or c-UNCD) thin films grown on a planar Si-substrate. The probable cause is that in the MPECVD process, the plasma cannot reach the bottom region of the SiNW arrays due to the closely packing of the SiNW arrays. The N_2-UNCD (or c-UNCD) films were not grown completely covering the bottom of the SiNW arrays. The electrons can only transport through resistive SiNWs to reach the tip of the UNCD/SiNW nanostructure materials for field emitting. Large resistance connected in series increases largely the turn-on field needed to

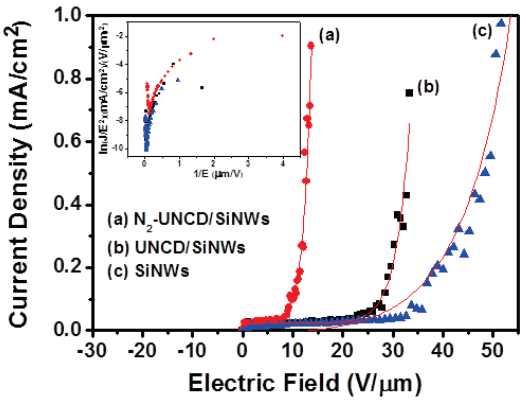

Fig. 8 The electron field emission properties of the UNCD films coated on the SiNW templates: (a) N_2-UNCD/SiNWs coated in CH_4/N_2 plasma at 700°C for 10 min and (b) conventional UNCD/SiNW coated in CH_4/Ar plasma at around 425°C for 60 min.

initiate the EFE process and suppressed the EFE current density. The probable ways for improving the EFE properties of these UNCD-coated SiNWs is utilization of more conducting Si-substrates for synthesizing the SiNWs, or increasing the spacing between the SiNW arrays that allows the plasma to reach the bottom region of the SiNWs to more uniformly grow UNCD films on the SiNW arrays. Moreover, larger spacing between the SiNWs in the arrays will increase the field enhancement factor for the UNCD/SiNWs that will further enhance the EFE process.

The plasma illumination characteristics of the plasma devices with capacity-type configuration (CP-devices), using UNCD/SiNW nanostructure materials as cathode and ITO as anode with 1 mm cathode-to-anode gap are shown in Fig. 9. This figure shows that the Ar plasma can be triggered at a low applied voltage of 210 V, which corresponds to a turn on field of 0.21 V/μm, regardless of the nature of the cathode materials. The plasma illumination current increases monotonously with the applied field. Detail analyses on these plasma illumination behaviors reveals a subtle advantages for using N_2-UNCD/SiNW nanostructure materials as cathode for the CP-devices, as compared with the c-UNCD/SiNW nanostructure materials cathoded ones. The plasma current density achieve around $(J_{pl})_{c\text{-}UNCD}$=3.2 mA/cm^2 at an applied field of E_a=0.35 V/μm when using c-UNCD/SiNW nanostructure materials as cathodes (Fig. 9(a)), whereas $(J_{pl})_{N2\text{-}UNCD}$=5.0 mA/cm^2 at the same applied field for N_2-UNCD/SiNWs cathoded devices (Fig. 9(b)). The larger plasma illumination current density for the N_2-UNCD/SiNWs cathoded device is apparently resulted from the larger EFE current density for these materials. Furthermore, both CP-devices cathoded with N_2-UNCD/SiNWs or c-UNCD/SiNW nanostructure materials shown markedly better plasma illumination behavior than those cathoded with uncoated SiNWs, i.e., $(E_{th})_{SiNWs}$=0.23 V/μm and $(J_{pl})_{SiNWs}$=2.0 mA/cm^2 (at an applied field of E_a=0.35 V/μm). The plasma illumination and EFE properties corresponding to SiNWs are summarized in Table I(b).

It should be noted that the plasma illumination of the CP-devices can be triggered when the electrons emitted from the cathode (e.g. UNCD/SiNWs) gained a sufficient kinetic energy for ionizing the gas molecules (15.7 eV for Ar-species). The ionization cross-section for Ar-species increases around 100 eV [25]. Therefore, although the EFE process for N_2-UNCD/SiNW arrays can be turned on at much lower field ($(E_0)_{N2\text{-}UNCD}$=7.8 V/μm), as compared with that for c-UNCD/SiNW ones, the onset field for triggering illumination process does not show much difference when the cathode materials were changed from N_2-UNCD/SiNW nanostructure materials to c-UNCD/SiNW ones. Only the plasma illumination current density was markedly larger for the CP-devices coathoded with the N_2-UNCD/SiNW nanostructure materials that, apparently, is owing to the possess larger EFE capacity for these materials.

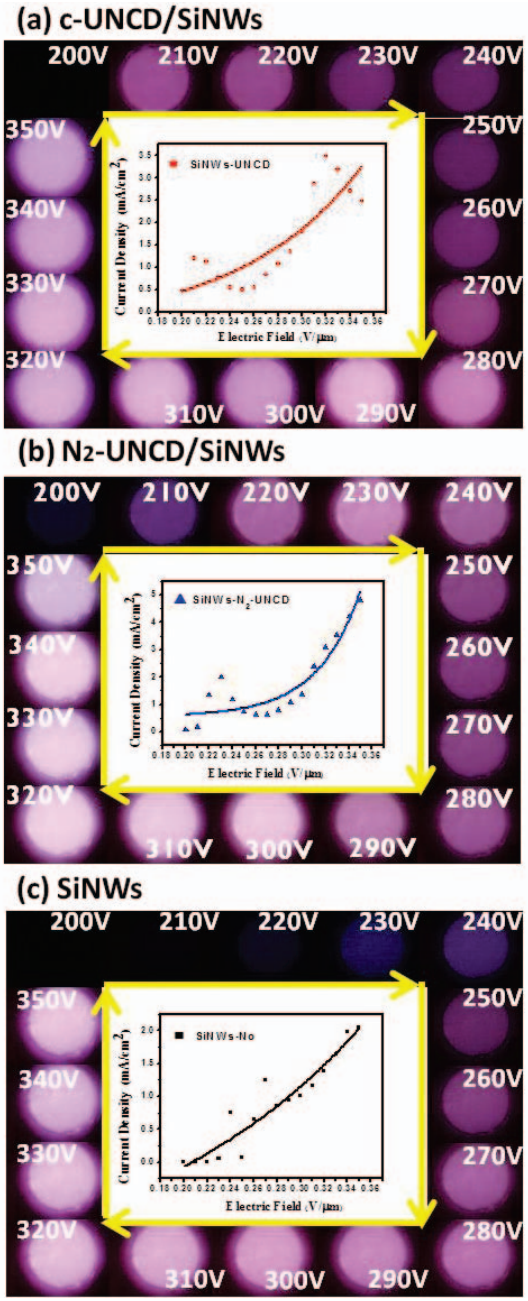

Fig. 9 The plasma illumination properties of CP-devices where the cathodes are the diamond coated on SiNW nanostructures: (a) N_2-UNCD/SiNWs grown in CH_4/N_2 plasma at 700°C for 10 min, (b) conventional UNCD/SiNW grown in CH_4/Ar plasma at around 425°C for 60 min and (c) the uncoated SiNW nanostructures.

IV. CONCLUSION

The effect of cathode materials on the plasma illumination characteristics of the a capacitive-type plasma devices (CP-devices) was systemtically examined. It is observed that the plasma illumination charateristics of the CP-devices is closely correlated with the electron field emission behavior of the cathode materials, which, in turn, was enhanced due to the improvement in conductivity of the UNCD films. The N_2-UNCD/SiNW nanostructure materials, which were grown in CH_4/N_2 plasma at 700°C possess markedly better conductivity ($\sigma_{N2\text{-}UNCD}$=2-3(Ω cm)$^{-1}$), as compared with the conventional c-UNCD/SiNWs ones, which were grown in CH_4/Ar plasma at around 425°C ($\sigma_{c\text{-}UNCD}$<0.01(Ω cm)$^{-1}$). The EFE process of the former materials can be turned on at $(E_0)_{N2\text{-}UNCD}$=7.80 V/μm achieving larger EFE current density of $(J_e)_{N2\text{-}UNCD}$=0.87 mA/cm^2 at an applied field of 13.0 V/μm, whereas that of the latter materials need $(E_0)_{=UNCD}$=18.25 V/μm to turn on, attaining only $(J_e)_{UNCD}$=0.024 mA/cm^2 at same applied field. While the plasma illumination process can be triggered at around 0.21 V/μm, regardless of the characteristics of the cathod materials, plasma illumination intensity/current density is larger when the materials with better EFE properties were used as cathodes for the plasma device. The plasma illumination current density is around $(J_{pl})_{N2\text{-}UNCD}$=5.0 mA/cm^2 (at an applied field of 0.35 V/μm when N_2-UNCD nanostructure materials was used as cathode, whereas the $(J_{pl})_{c\text{-}UNCD}$=3.2 mA/cm^2 when the conventional c-UNCD/SiNW nanostructure materials was used as cathode.

ACKNOWLEDGMENTS

The authors appreciate the financial support from the National Science Council through the project No. NSC 99-2119-M-032- 003-MY2.

REFERENCES

[1] K. Chakrabarti, R. Chakrabarrti, K.K. Chattopadhyay, S.Chaudhrui, and A.K. Pal, "Nano-diamond films produced from CVD of camphor," Diamond Relat. Mater., vol. 7, pp.845-852, 1998.

[2] V. Ralchenko, A. Karabutov, I. Vlasov, V. Frolov, V. Konov, S. Gordeev, S. Zhukov, and A. Dementjev, "Diamond–carbon nanocomposites: applications for diamond film deposition and field electron emission," Diamond Relat. Mater., vol. 8, pp.1496-1501, 1999.

[3] S. G. Wang, Q.Zhan, S.F. Yoon, J. Ahn, Q. Wang, Q.Zhou, and D.J.Yang, "Electron field emission propertiesof nano-, submicro- and micro-diamond films," Phys. Stat. Sol. (a), vol. 193, pp.546-551, 2002.

[4] D. M. Gruen, "Nanocrystalline diamond film 1," Annu. Rev. Mater. Sci. vol. 29, pp. 211-259, 1999.

[5] J. A. Carlisle, and O. Auciello, "Ultrananocrystalline Diamond," Electrochem. Soc. Interface Spring, pp. 28-31, 2003.

[6] Y. C. Lee, S. J. Lin, C. T. Chia, H. F. Cheng, and I. N. Lin, "Synthesis and electron field emission properties of nanodiamond films," Diam. Relat. Mater., vol. 13, pp. 2100-2104, 2004.

[7] D. Pradhan, Y. C. Lee, C. W. Pao, W. F. Pong, and I. N. Lin, "Low temperature growth of ultrananocrystalline diamond film and its field emission properties," Diam. Relat. Mater., vol. 15, pp. 2001-2005, 2006.

[8] Y.C. Lee, S.J. Lin, D. Pradhan, and I.N. Lin, "Improvement on the growth of ultrananocrystalline diamond by using pre-nucleation technique," Diam. Relat. Mater., vol. 15, pp. 353-356, 2006.

[9] S.J. Park, J. Chen, C. J. Wagner, N. P. Ostrom, C. Liu, and J. G. Eden, "Microdischarge arrays: a new family of photonic devices," IEEE J. Sel. Top. Quantum Electron.vol. 8, pp. 387-394, 2002.

[10] S.J. Park, J. G. Eden, J. Chen, and C. Liu, "Microdischarge devices with 10 or 30 μm square silicon cathode cavities: pd scaling and production of the XeO excimer," Appl. Phys. Lett. vol. 85, pp. 4869-4871, 2004.

[11] S.J. Park, K.-F. Chen, N. P. Ostrom, and J. G. Eden, "40 000 pixel arrays of ac-excited silicon microcavity plasma devices," Appl. Phys. Lett. vol. 86, pp. 111501-111501-3 , 2005.

[12] K. H. Becker, K. H. Schoenbach, and J. G. Eden, "Microplasmas and applications," J. Phys. D, vol. 39, R55-R70, 2006.

[13] K. H. Schoenbach, R. Verhappen, T. Tessnow, P. F. Peterkin, and W. W. Byszewski, "Microhollow cathode discharges," Appl. Phys. Lett. vol. 68, pp. 13-15, 1996.

[14] J. W. Frame, D. J. Wheeler, T. A. DeTemple, and J. G. Eden, "Microdischarge devices fabricated in silicon," Appl. Phys. Lett. vol. 71, pp. 1165-1167, 1997.

[15] S.J. Park and J. G. Eden, "13–30 micron diameter microdischarge devices: Atomic ion and molecular emission at above atmospheric pressures," Appl. Phys. Lett. vol. 81, pp. 4127-4129, 2002.

[16] C. Penache, M. Miclea, A. Bräuning-Demian, O. Hohn, S. Schössler, T. Jahnke, K. Niemax, and H. Schmidt-Böcking,

"Characterization of a high-pressure microdischarge using diode laser atomic absorption spectroscopy," Plasma Sources Sci. Technol. vol. 11, pp. 476-483, 2002.

[17] K.F. Chen, N. P. Ostrom, S.-J. Park, and J. G. Eden, "One quarter million (500×500) pixel arrays of silicon microcavity plasma devices: Luminous efficacy above 6 lumens/watt with Ne/50% Xe mixtures and a green phosphor," Appl. Phys. Lett. vol. 88, pp. 061121-061121-3, 2006.

[18] W. Kern, "The evolution of silicon wafer cleaning technology," J. Electrochem. Soc. vol. 137, pp. 1887-1892, 1990.

[19] Y.F. Tzeng, Y.C. Lee, C.Y. Lee, I.N. Lin, and H.T. Chiu, "On the enhancement of field emission performance of ultrananocrystalline diamond coated nanoemitters," Appl. Phys. Lett. vol. 91, pp. 063117-063117-3, 2007.

[20] R. H. Fowler, L. Nordheim, "Electron emission in intense electric fields," Proc. R. Soc. A, vol. 119, pp. 173-181, 1928.

[21] J. Michler, Y. Von Kaenel, J. Stiegler, and E. Blank, "Complementary application of electron microscopy and micro-Raman spectroscopy for microstructure, stress, and bonding defect investigation of heteroepitaxial chemical vapor deposited diamond films," J. Appl. Phys. vol. 81, pp. 187-197, 1998.

[22] A. C. Ferrari and J. Robertson, "Interpretation of Raman spectra of disordered and amorphous carbon," Phys. Rev. B vol. 61, pp. 14095-14107, 2000.

[23] Z. Sun, J. R. Shi, B. K. Tay, and S. P. Lau, "UV Raman characteristics of nanocrystalline diamond films with different grain size," Diamond Relat. Mater. vol. 9, pp. 1979-1983, 2000.

[24] A. C. Ferrari and J. Robertson, "Origin of the 1150-cm^{-1} Raman mode in nanocrystalline diamond," Phys. Rev. B vol. 63, pp. 121405-121405-4, 2001.

[25] H. F. Cheng, H. Y. Chiang, C. C. Horng, H. C. Chen, C. S. Wang, and I. N. Lin, "Enhanced electron field emission properties by tuning the microstructure of ultrananocrystalline diamond film," J. Appl. Phys. vol. 109, pp. 033711-033711-8, 2011.